High-Performance MAPbI3-Based Perovskite Solar Cell: Design, Simulation, and Analysis of Optoelectronic Properties and Efficiency Metrics Using SILVACO TCAD

Md. Rashique Hamjah Chowdhury
ORCID: http://orcid.org/0009-0008-6642-1189
United International University, Dhaka, Bangladesh
E-mail: mchowdhury212168@bscse.uiu.ac.bd
Md. Hojaifa Daiyan Chowdhury
ORCID: http://orcid.org/0009-0003-4858-8122
United International University, Dhaka, Bangladesh
E-mail: mchowdhury203072@bscse.uiu.ac.bd
Muhammad Johirul Islam
ORCID: http://orcid.org/0000-0001-8694-6187
United International University, Dhaka, Bangladesh
E-mail: johir021@yahoo.com
Md. Iqbal Bahar Chowdhury
ORCID: http://orcid.org/0000-0001-8563-6267
United International University, Dhaka, Bangladesh
E-mail: iqbal@eee.uiu.ac.bd

Abstract
In this work, a perovskite solar cell (PSC) based on MAPbI3 has been designed, modeled, implemented, investigated and analyzed in Silvaco TCAD environment. A thin layer of MAPbI3 serves as the photoactive absorber. A thinner layer of PEDOT: PSS based organic material acts as the hole transport layer to enhance the hole transport towards the ITO electrode and a thin layer of ZnO based inorganic material serves as the electron transport layer to assist electron transport to the aluminum electrode. Simulations have been carried out to obtain the energy band diagram and the electric field profile as well as the contour and 2D plots of photon absorption rate, the recombination rate and the photogeneration rate to gain a physical insight of electronic and optical behavior of the proposed solar cell. The current-voltage (JV) characteristics and the external quantum efficiency (EQE) of the device are also plotted. The deduced performance metrics of the proposed PSC demonstrates a short circuit current density (JSC) of 27.247 mA/cm^2, an open circuit voltage (VOC) of 0.978 V, a fill factor (FF) of 71.80% and a power conversion efficiency (PCE) of 21.25%, where the EQEs with and without considering the whole device absorption is more than 30% and 50% respectively over the visible and infra-red wavelength range (0.3 μm -1.0 μm).
Keywords: Perovskite solar cell, MAPbI3, PEDOT: PSS, ZnO, ITO, Silvaco TCAD, PCE.

1. Introduction

The solar energy, an environmentally-harmless (Nayak *et al*., 2019) resource of energy, can supply a huge energy- 4 million exajoule per year (Kabir *et al*., 2017; Ho *et al*., 2024). This ample energy can be harvested by the photovoltaic cells, commonly known as solar cells. Till 2021 solar panels covered 28% of total global capacity (Ho *et al*., 2024; Nowsherwan *et al*., 2023). Solar cells

also have the potential to deal with the climactic change enhanced by the global warming through carbon neutralization (Nowsherwan *et al*., 2023). Theoretically, the maximum power conversion efficiency (PCE) that can be achieved by the solar cells is ≈ 33% (known as Schockley-Quisser limit (Guillemoles *et al*., 2019)). To achieve this limit with reduced material and fabrication cost seamless research endeavors have been conducted in the scientific community by utilizing different low-cost absorber materials with different structures which lead the evolution of different generations of solar cells (i.e., 1G, 2G, 3G). The 1G cells, the most primitive generation, involve costlier crystalline silicon (Si) and silicon-derived (i.e., SiGe) materials with p-n junction- and metal-insulator-semiconductor (MIS) junction-based structures (M. J. Islam *et al*., 2016) and achieved a PCE of ≈ 25%. The PCE of p-n junction structured 1G solar cells can be further enhanced by developing a drift field in the absorber layer through the use of heavily and non-uniformly doping there in (Huqe *et al*., 2013; S. K. Saha, Farhan, *et al*., 2011; S. K. Saha, Ferdaus, *et al*.2011; N. S. K. Saha, Ferdaus, *et al*., 2011; Huqe & Chowdhury, 2016; Huqe *et al*., 2012). For MIS solar cells, use of low-cost materials (i.e., GaAs) have the promise of enhanced PCE with reduced cost. In 2G generation, the cell's higher PCE with significantly lower cost is ensured by employing a number of earth-abundant materials such as such as amorphous Si (M. I. Chowdhury *et al*., 2020), CdTe (Haque *et al*., 2014b; Biswas *et al*., 2015; Rivon *et al*., 2016), CIGS (Haque *et al*., 2014a; Rahim *et al*., 2015; M. J. Islam *et al*., 2024), CZTS (Ayesha *et al*., 2016; Nikita *et al*., 2016) and CZTSSe (Hasan & Chowdhury, 2018). The fabrication cost of all these solar cells has been significantly reduced. The quantum well (Barnham & Duggan, 1990; M. J. Islam & Chowdhury, 2024; Nabiah *et al*., 2024; Mostafa *et al*., 2020; M. J. Islam *et al*., 2020; Johir *et al*., 2021; M. I. Chowdhury & Mostafa, 2020) and quantum dot (Aroutiounian *et al*., 2001; Aissat *et al*., 2016; Bi *et al*., 2016; Nawaz *et al*., 2023) based solar cells have been also reported with the promise of higher PCE with reduced cost. Low-cost, abundant materials such as organic semiconductors (W. H. Chowdhury *et al*., 2021; Chakma *et al*., 2024; M. R. H. Chowdhury *et al*., 2024), dyes (O'Regan & Grätzel, 1991; Rahman *et al*., 2023; Benesperi *et al*., 2018; M. N. Islam *et al*., 2024) and perovskite semiconductors (Chen *et al*., 2023; Pitaro *et al*., 2021; Jeon *et al*., 2018; Herz, 2017; T. A. Chowdhury *et al*., 2023) are used as the absorber materials in 3G solar cells- all of which involves low-energy, roll-to-roll, solution-processible manufacturing process thereby enabling low-cost fabrication process (Ho *et al*., 2024).

Perovskite semiconductor-based solar cell, termed hereafter as PSC, is the fastest-growing 3G technology (Ho *et al*., 2024), as the PCE of PSCs steeply rises from 3.8% (first invented in 2009 (Kojima *et al*., 2009)) to more than 25% (reported recently) (Park *et al*., 2023)). This steep rise in PCE can be attributed to the excellent structural (higher crystallinity, ionicity, and defect tolerance) (Ho *et al*., 2024), electronic (higher relative permittivity, lower exciton binding energy, higher carrier mobility, and larger carrier diffusion length) (Chen *et al*., 2023), and optical (higher absorption coefficient) properties (Pitaro *et al*., 2021). PSCs are appropriate for indoor applications owing to their increased PCE under reduced illumination (Wu *et al*., 2021). They can be used in portable and wearable electronics due to their ability of fabrication on flexible substrates (Tebbal & Hamida, 2023). They are superior choice in building-integrated photovoltaic (BIPV) applications (Bati *et al*., 2023). In a typical planar regular PSC structure, the perovskite semiconductor is sandwiched between a hole transport layer (HTL) and an electron transport layer (ETL), where a transparent conductive oxide (i.e., ITO, FTO) next to HTL and a metal contact (i.e., aluminum, silver) next to ETL serve as the anode and the cathode respectively. The common HTLs are spiro-OMeTAD, PEDOT: PSS and NiO (Ho *et al*., 2024), whereas, ZnO, tin oxide (SnO_2) and titanium oxide (TiO_2), are preferrable ETLs (Chen *et al*., 2023). Of various perovskite semiconductors reported till to date, Methylammonium lead iodide (MAPbI3) is more preferrable because of its excellent electrical and optical properties, low-temperature solution processability, long lifetime, and ferroelectricity (Husainat *et al*., 2019).

This work aims to design and investigate a perovskite solar cell (PSC) in the Silvaco TCAD environment, as it is more versatile and has the ability to incorporate almost all the physics-based

models and hence, is a suitable tool to analyze complex structures (Hossain *et al.*, 2014). The intended solar cell uses MAPbI3 as the perovskite absorber, PEDOT: PSS as the HTL (owing to its ability to enhance solar cell functioning (Murugesan *et al.*, 2015)), ZnO as the ETL (owing to its outstanding electronic and optical properties and affordable processing (Bati *et al.*, 2023)), ITO as the front electrode and aluminum as the back electrode.
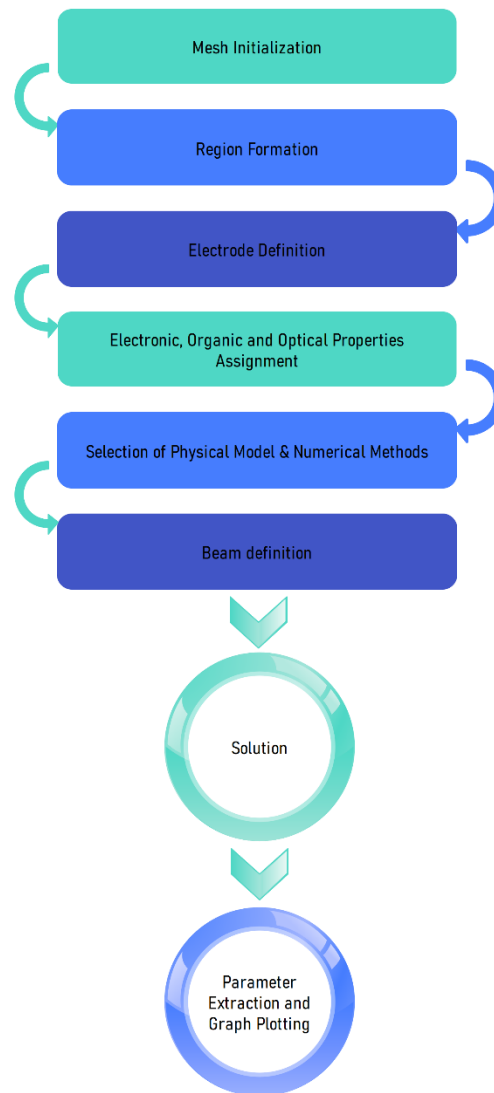
2. Methodology

Figure 1 - Flowchart of Silvaco Atlas based solar cell modeling.

This work employs Atlas tool of Silvaco TCAD to model and simulate the proposed PSC. The first step is crucial to balance between the accuracy and the simulation time. Fine meshing has better accuracy with increased simulation time, whereas, course meshing reduces the simulation time at the cost of accuracy (M. R. H. Chowdhury *et al.*, 2024). The regions, electrodes and contacts are defined in the next two steps. Next, the electronic, organic and optical properties of each layer material are defined based on the literature. Electronic properties must include bandgap, permittivity, affinity, effective density of states in the conduction band (EC), effective density of states in the valence band (EV), electron mobility (μn) and hole mobility (μp), organic properties include relevant parameters for singlet dissociation and recombination as well as Langevin

recombination and optical properties include wavelength-dependent refractive index and extinction coefficient. In the following step, appropriate physical models (the most important one) and numerical methods are chosen. Specification of the solar irradiation profile in the next step completes the design of the PSC. Afterwards, the PSC has been simulated under illumination and bias conditions. Finally, simulation results are extracted to obtain the performance metrics and also, necessary graphs are plotted.

3. Structure and Simulation

In this work, a reference structure implemented in SCAPS 1D and reported in Husainat *et al*. (2019) has been modified to enhance the PCE. The reference PSC structure is based on FTO/TiO$_2$/ MAPbI3/Spiro-OMETAD/Au with a PCE of 20.34%, where MAPbI3 is used as the absorber layer (thickness is 300 nm), TiO$_2$ as the ETL, Spiro-OMETAD as the HTL, FTO is the front electrode and Au (gold) as the back electrode. Severe recombination has been observed between the perovskite films and the FTO electrode in the presence of pinholes in TiO$_2$ layers leading to poor performance (Ho *et al*., 2024). Therefore, ZnO is proposed as ETL in this work to improve performance. Spiro-OMeTAD has inherent stability problem, Bati *et al*. (2023), whereas, PEDOT: PSS enhances solar cell functioning (Murugesan *et al*., 2015). Hence, PEDOT: PSS is better alternative as HTL than Spiro-OMeTAD for improved cell stability. Au is a costlier metal than aluminum (Al) and hence, use of Al can reduce the cost. Therefore, the proposed PSC in this work has been modified to a structure of ITO/PEDOT: PSS/ MAPbI3/ZnO/Aluminum to enhance the PCE, reduce the cost and improve the cell stability.
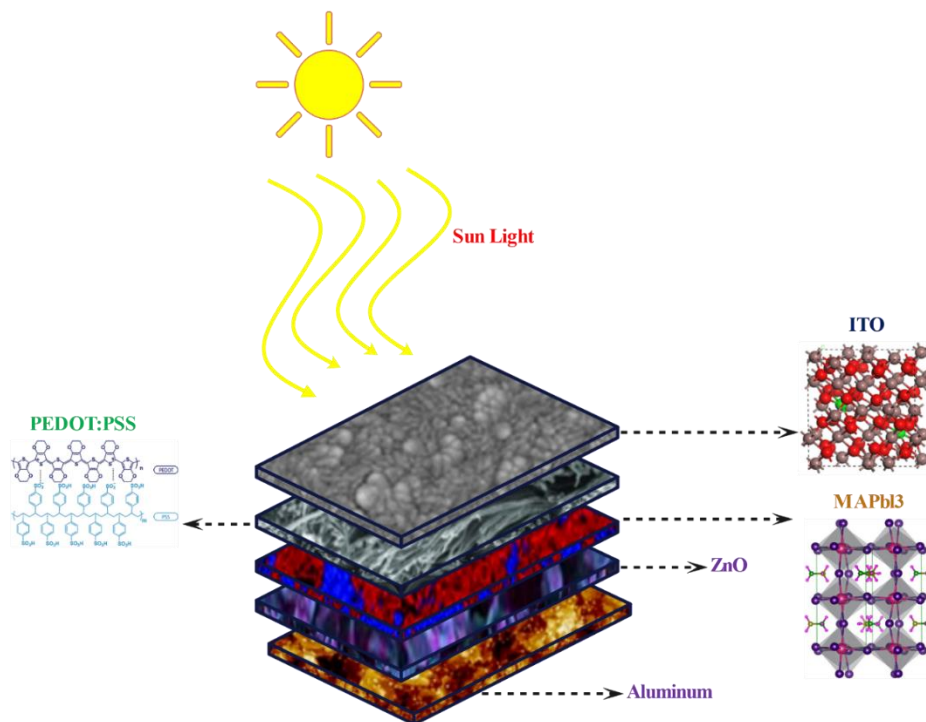

Figure 2 - The proposed structure of MAPbI3 based PSC.

Figure 2 shows the schematic of the proposed PSC structure investigated in this work. The photoactive absorber layer MAPbI3 is sandwiched between the top PEDOT: PSS HTL and the bottom ZnO ETL, ITO and aluminum are used as the front and back electrodes. The dimensions of all these materials are shown in Table 1. The electronic properties of MAPbI3, PEDOT: PSS and ZnO are listed in Table 2. Work function values of ITO and aluminum are chosen as 4.8 eV and 4.1 eV respectively. The optical properties i.e., the refractive index and the extinction coefficient have been collected from literature (RefractiveIndex.INFO - Refractive Index Database, n.d.). As incident

solar irradiation, the terrestrial solar spectral irradiance specified by the American Society for Testing and Materials (ASTM) G-173 (Reference Air Mass 1.5 Spectra, n.d.) has been used.

Table 1 –Layer, Material, and thickness for proposed PSC structure.

Layer	Material	Thickness
Front Electrode	ITO	120 nm
HTL	PEDOT: PSS	30 nm
Absorber	MAPbI3	300 nm
ETL	ZnO	200 nm
Back Electrode	Aluminum	100 nm

Table 2: Electronic properties of different layer materials used in the proposed PSC.

Electronic Property	MAPbI3	PEDOT: PSS	ZnO
Bandgap (eV)	1.5	1.6	3.37
Permittivity	3.9	3.0	9.0
Affinity (eV)	30	3.5	4.54
Nc (cm-3)	2.5×1020	5.0×1019	2.2×1018
Nv (cm-3)	2.5×1020	5.0×1019	1.8×1019
μn (cm2/V-sec)	50	0.1	100
μp (cm2/V-sec)	50	0.08	25
Work function (eV)	-	-	

The proposed structure has been implemented in the Silvaco TCAD environment. The modeling includes Fermi statistics, and SRH, Auger and optical recombination mechanisms. Since MAPbI3 and PEDOT: PSS are not defined in Silvaco TCAD, the user-defined material option of TCAD is used; MAPbI3 is defined as 'polysilicon' and PEDOT: PSS is defined as 'organic'. The 2D view of the proposed PSC structure, implemented in Silvaco TCAD, is shown in Figure 3.
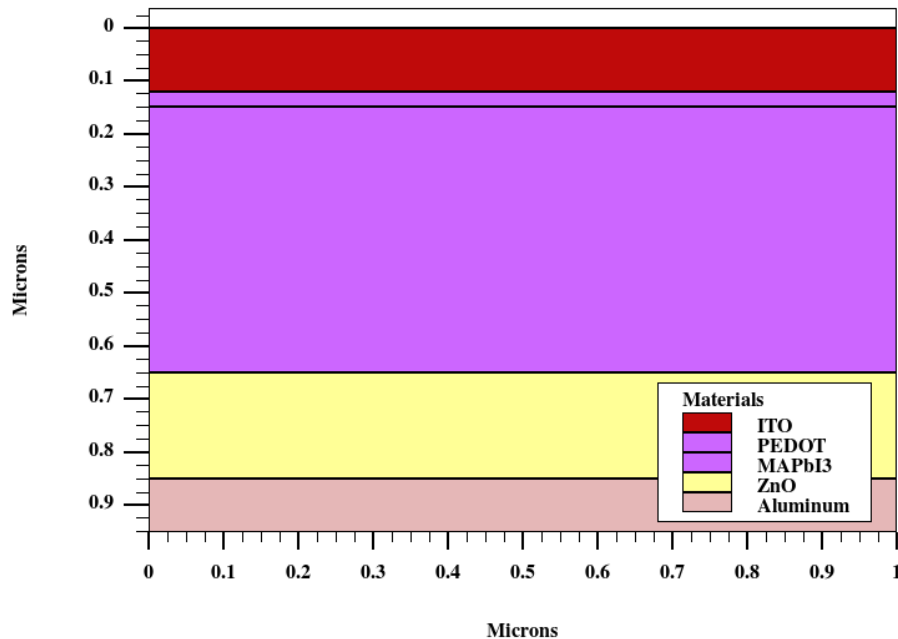

Figure 3 - Silvaco TCAD-implemented structure of the proposed PSC.

4. Results and Discussion

This section presents, analyses and discusses the simulation results obtained from TCAD simulation of the proposed PSC structure. These results include the plots of energy band diagram, electric field, photon absorption rate, recombination rate and photogeneration rate. Internal and external quantum efficiencies (IQE and EQE) and current-voltage (JV) characteristics of the proposed PSC are also presented. Finally, various performance metrics which include short circuit current density (JSC), open circuit voltage (VOC), fill factor (FF) and PCE of the proposed PSC are presented and compared with the reference structure reported in Husainat *et al*. (2019). Figs. 4(a) and 4(b) present the energy band diagram and the electric field profile respectively of the proposed PSC under zero-bias and no light condition. The vertical lines separate the layer materials, where ITO, PEDOT: PSS, MAPbI3, ZnO and Al are presented from left to right. The linearity of the conduction and valence band energies observed in MAPbI3 layer represents its undoped nature, for which electric field in this layer becomes constant, as seen from Figure 4(b). The discontinuity in the energy bands observed at the interfaces is due to the work function difference between the materials involved at each interface. This discontinuity results in a depletion region near each interface, for which energy bands are bent [Figure 4(a)] and nonuniform electric field has been developed [Figure 4(b)] near these interfaces. The observed higher level of electric field in the absorber layer confirms the efficient electron-hole separation of the excitons photogenerated therein. The even higher field observed at the interfaces of ITO/ PEDOT: PSS and ZnO/Al helps improved charge carrier extraction towards the electrodes.
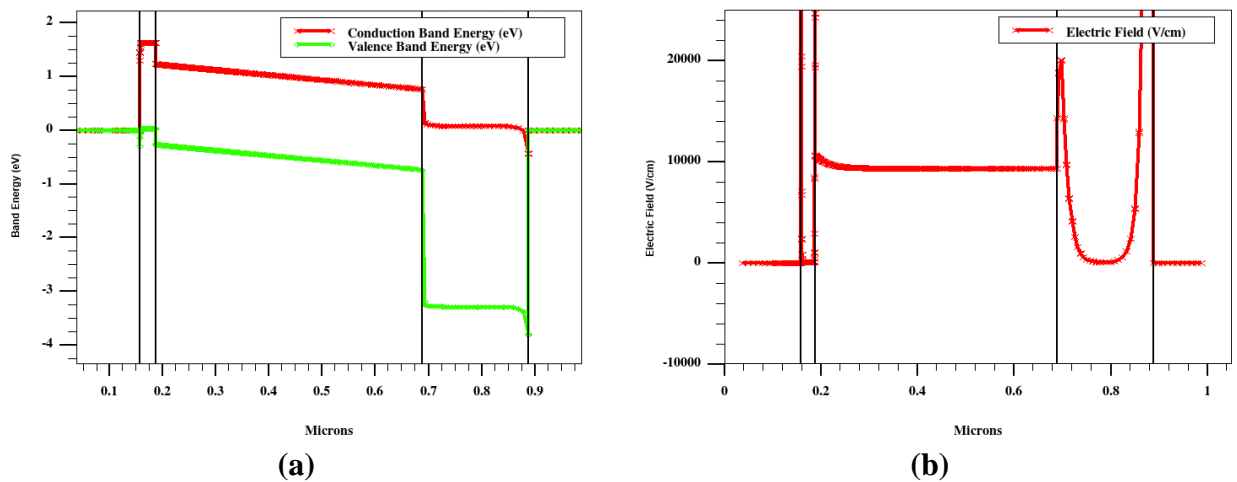

(a)   **(b)**

Figure 4 - (a) Energy band diagram and (b) Electric field profile of the proposed PSC.

The contour and 2D views of the photon absorption rate under no bias condition are presented in Figs. 5(a, b). These plots reveal that the photons are mostly absorbed in the MAPbI3 layer. This absorption is almost exponential, which peaks at the interface with the PEDOT: PSS layer and exponentially decays as moves toward the ZnO layer. Figs. 5(a, b) also shows a small amount of absorption in the PEDOT: PSS and ZnO layers.
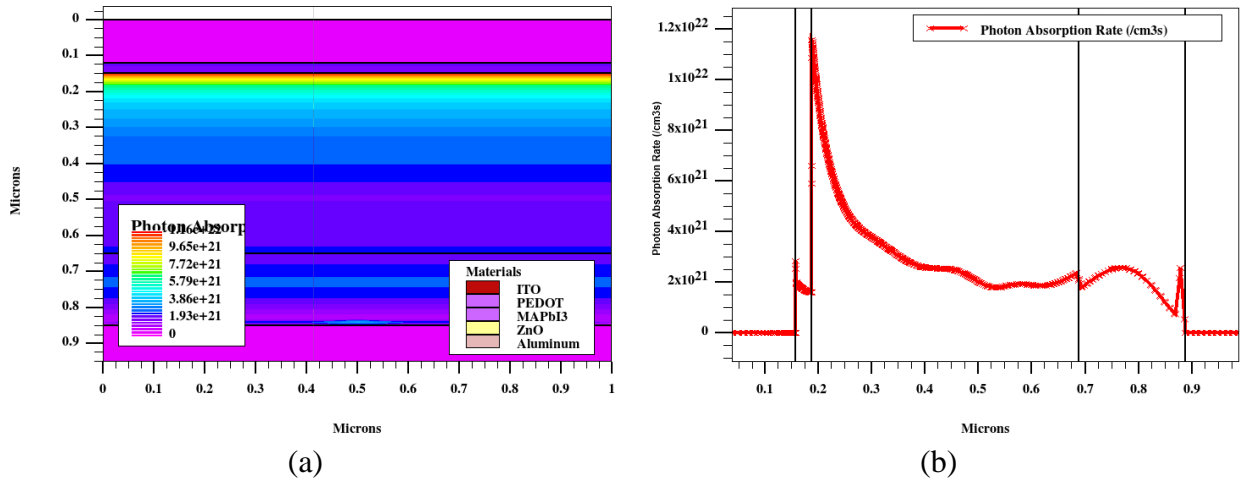
(a)   (b)

Figure 5 - (a) Contour and (b) 2D plot of the photon absorption rate in the proposed PSC.

The contour and 2D plots in Figure 6 present the recombination rate in the different layers of the proposed PSC. These plots show that the recombination of carriers happens in all three layers of absorber, HTL and ETL. The highest recombination happens in the ETL, lowest in the HTL, and in between in the absorber layer. This means that the mismatch between the absorber and ETL is the highest and that between the absorber and HTL is the lowest, whereas, almost constant recombination in the absorber reveals its structural uniformity.
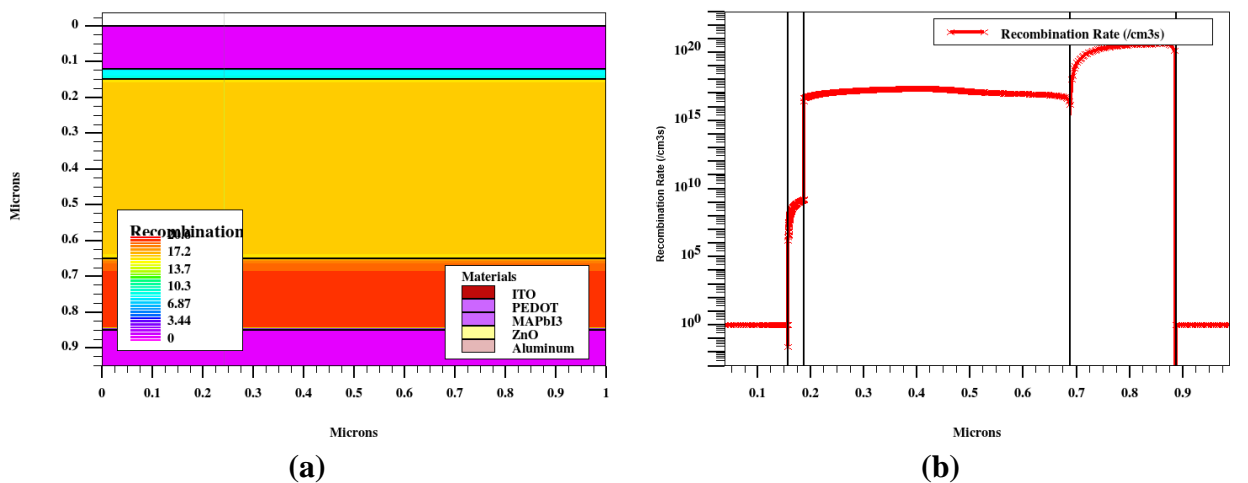

(a)   (b)

Figure 6 - (a) Contour and (b) 2D plot of the recombination rate in the proposed PSC.

The contour and 2D plots of the photogeneration rate in the different layers of the proposed PSC are presented in Figure 7. Both these plots reveal that the highest photogeneration occurs in the MAPbI3 absorber layer, which almost exponential decays from left to right. A comparatively smaller photogeneration also occurs in the ZnO layer. However, no photogeneration is happened in the PEDOT: PSS layer.
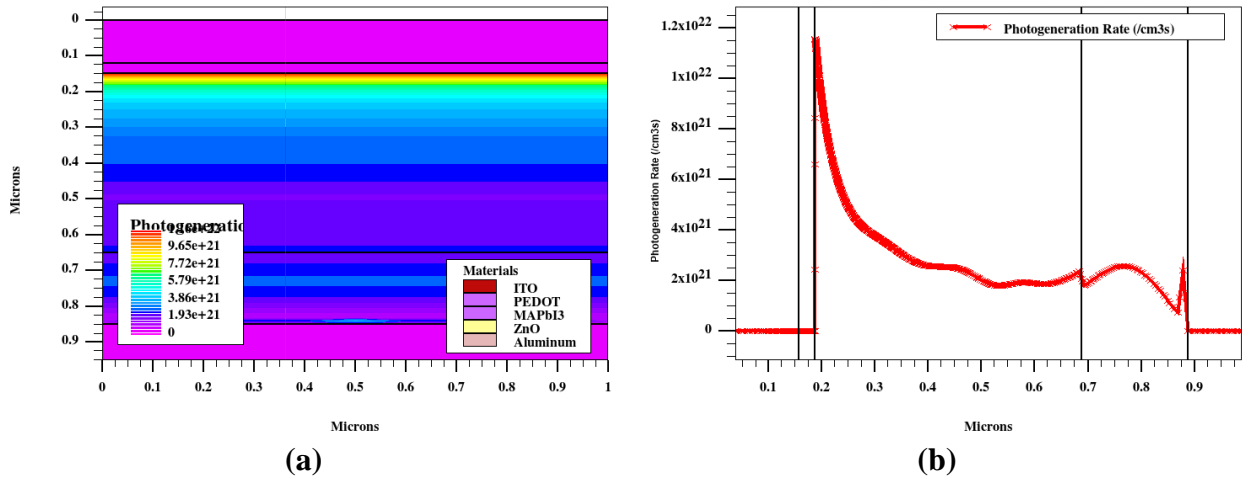
Figure 7 - (a) Contour and (b) 2D plot of the photogeneration rate in the proposed PSC.

The reflection, transmission and absorption spectra of the proposed PSC over a wavelength range 0.3 μm-1.0 μm are presented in the plots of Figs. 8(a-c). The reflection is < 30% for wavelengths up to 0.75 μm, then starts to rise and reaches ≈ 50% at a wavelength of 0.98 μm, as seen from Figure 8(a). On the other hand, Figure 8(b) shows that the transmission is zero for wavelengths up to 0.52 μm and then increases, however, it remains < 0.24%. As seen from Figure 8(c), the absorption is > 50% over all the wavelength span and it is > 70% for wavelengths up to 0.76 μm. The lower reflection and transmission and the higher absorption over most of the wavelength span shows higher photon absorption capability of the proposed PSC.
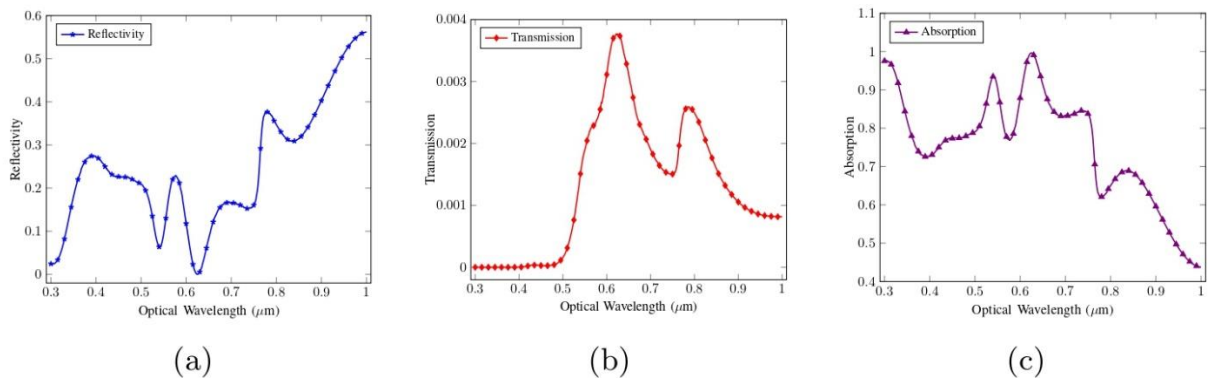

Figure 8 - (a) Reflection, (b) transmission and (c) absorption profile of the proposed PSC.

Figure 9 plots the variation of three photo-generated currents, namely source (IS), available (IA) and load (IL) against over the wavelength span of the irradiated solar spectrum. These currents are calculated based on the consideration of optical and electrical losses- IS does not consider any one, IA considers only the optical one and IL considers both Johir *et al*. (2021), where reflection and transmission losses from the optical loss and recombination of charge carriers form electrical loss. As seen from Figure 9, the optical loss is more severe than the electrical losses, as IA is significantly reduced from IS, whereas, IA and IL are very close throughout the wavelength range. This means that the reflection is higher and the recombination is lower in the proposed PSC.
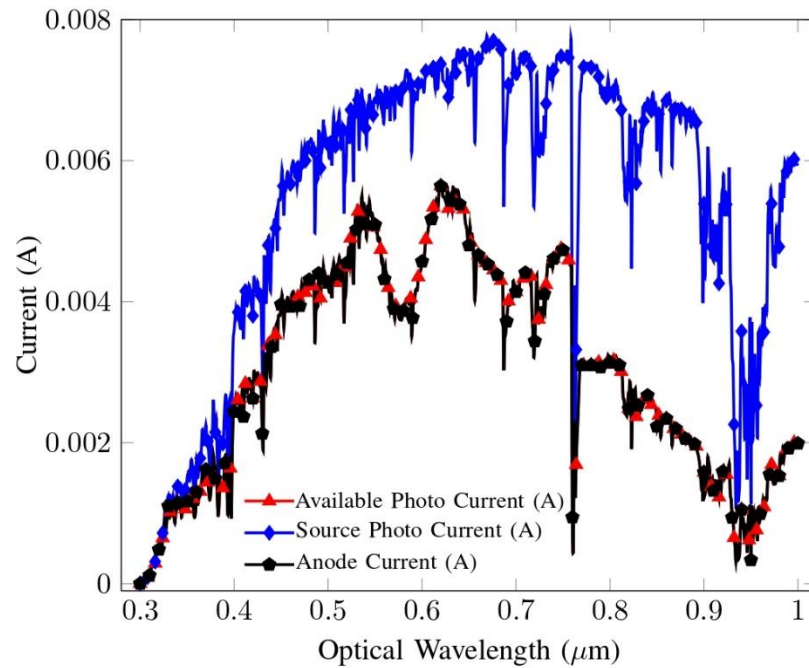
Figure 9 - The current profiles Vs. wavelength of the proposed PSC.

The IQE (ηint) and EQE (ηext1 and ηext2) plots of the proposed PSC are presented in Figure 10, where these quantities can be defined in terms of IS, IA, IL and absorption (A) as Johir *et al.* (2021):

$$\eta_{int} = \frac{I_L}{I_A}$$
$$\eta_{ext1} = \frac{I_L}{I_S}$$
$$\eta_{ext2} = \frac{I_L}{I_S A}$$

The IQE plot observed in Figure 10 approaches to 100% over the full wavelength of interest, as IL and IA are very close as observed in Figure 9 due to reduced recombination. On the other hand, the EQE plots have been observed severely degraded in the most part of the wavelength spans of interest. Since the absorption spectra is > 50% up to the wavelength of 0.76 μm, the EQEs are observed higher (>60%) in this span. However, EQE2 which considers absorption of the whole device becomes lower than EQE1 at the wavelengths > 0.55 μm and > 0.78 μm, meaning that parasitic absorption in the HTL and ETL increases at these wavelengths.
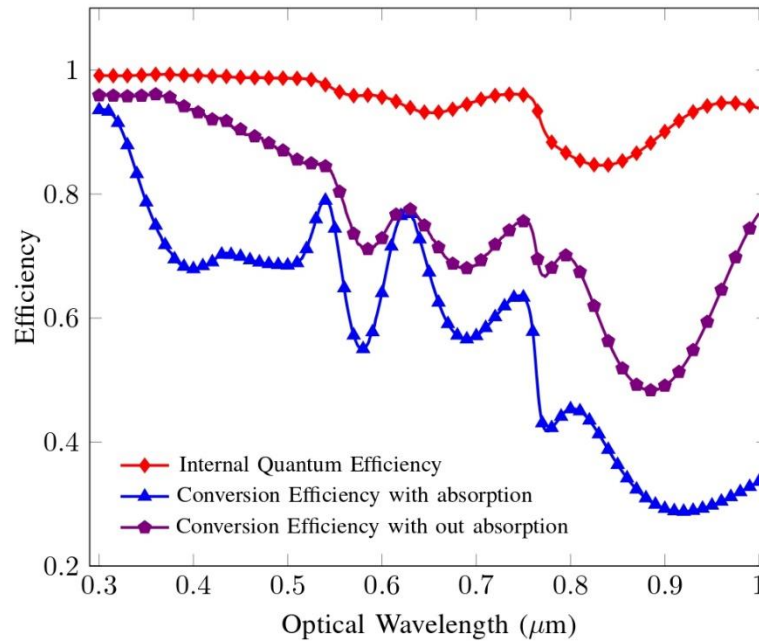
Figure 10 - IQE and EQE characteristics of the proposed PSC.

Figure 11 represents the JV characteristics curve of the proposed PSC. This curve closely resembles to typical square-like shape observed in inorganic solar cells, as reported in the literature (M. I. Chowdhury *et al*., 2020; Haque *et al*., 2014b; Biswas *et al*., 2015; Rivon *et al*., 2016; Haque *et al*., 2014a; Rahim *et al*., 2015; M. J. Islam *et al*., 2024; Ayesha *et al*., 2016; Nikita *et al*., 2016; Hasan & Chowdhury, 2018) and follows the two-diode model (A. Islam & Chowdhury, 2014) of inorganic solar cells. This typical inorganic JV behavior results in higher fill factor (FF) ($> 70\%$) of the proposed PSC, which is also reflected in Table 4.
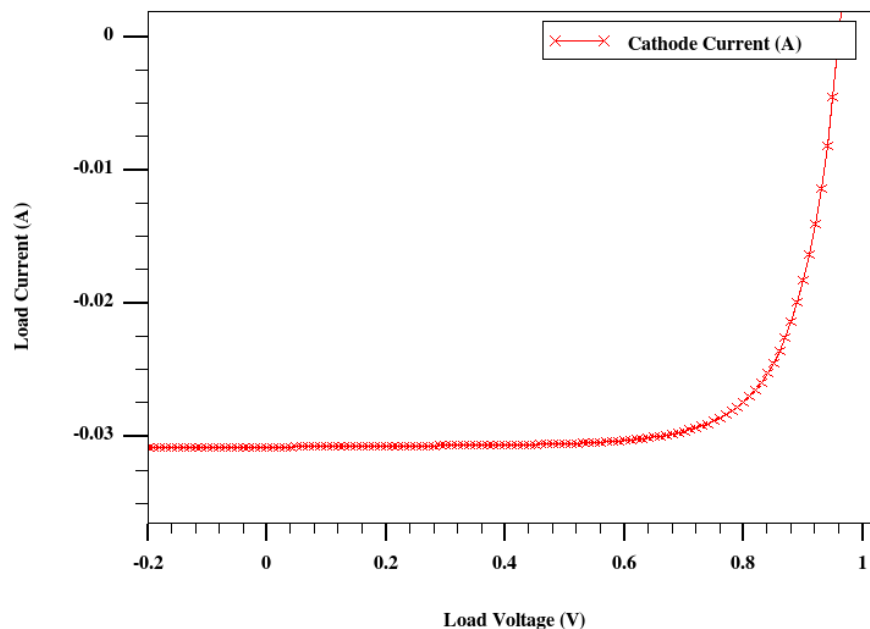

Figure 11 - JV characteristics of the proposed PSC.

The performance metrics comparison of the proposed PSC with the reference structure reported in (Husainat *et al*., 2019) has been presented in Table 4. The proposed PSC has much higher short circuit current density (JSC) than the reference cell, which reflects its better charge carrier collection. However, owing to the increased recombination in ZnO ETL, the open circuit voltage (VOC) and the FF of the proposed PSC becomes lower than the reference cell. However, the significant increase in JSC outperforms the decreased VOC and FF, resulting in the higher PCE of the proposed PSC.

Table 4: Performance metrics comparison of the proposed PSC with the reference structure (Husainat *et al*., 2019).

Performance Metrics	FTO/TiO$_2$/MAPbI3/SiproOMeTAD/Au (Husainat *et al*., 2019)	ITO/PEDOT: PSS/MAPbI3/ZnO/Al (This work)
Jsc (mA/cm^2)	15.158	27.247
Voc (V)	1.476	0.978
FF (%)	91	71.80
PCE (%)	20.34	21.25

5.Conclusion

In this work, an MAPbI3-based perovskite solar cell has been designed, modeled, and investigated for improved performance. The MAPbI3-based absorber layer is sandwiched between two electrodes (ITO and aluminum). The PEDOT: PSS placed atop of this absorber layer serves as the hole transport layer and enhances the hole transport to the ITO electrode. Instead of TiO$_2$, ZnO is used as an electron transport layer to overcome the recombination problem associated with the presence of pinholes in TiO$_2$. ITO and aluminum are used two electrodes. The proposed solar cell has been implemented and simulated in the Silvaco TCAD environment. Compared to the reported values in the literature, the proposed structure shows an increased PCE of 21.25% with significantly enhanced short-circuit current density (JSC) of 27.247 mA/cm^2. This significant improvement in JSC counterbalances the less values of open circuit voltage and fill factor as compared to the reported ones in the literature. The analysis regarding the degraded external quantum efficiency of the proposed PSC suggests that the continued research endeavors should be conducted to reduce the optical losses and hence, to enhance the PCE further.

References

Aissat, A., Benyettou, F., & Vilcot, J. P. (2016). Modeling and simulation of InGaN/GaN quantum dots solar cell. AIP Conference Proceedings, 1758, 030014. https://doi.org/10.1063/1.4959410

Aroutiounian, V. M., Petrosyan, S., Khachatryan, A., & Touryan, K. J. (2001). Quantum Dot Solar cells. Proceedings of SPIE, the International Society for Optical Engineering/Proceedings of SPIE, 4458, 38–45. https://doi.org/10.1117/12.448264

Ayesha, N., Kulsum, N., Silvi, S. K., & Chowdhury, M. I. B. (2016). Modeling of J-V characteristics of CZTS based thin film solar cells including voltage and space dependent electric field in the absorber layer. In 4th International Conference on the Development in the in Renewable Energy Technology (ICDRET) (pp. 1–4). https://doi.org/10.1109/icdret.2016.7421486

Barnham, K. W. J., & Duggan, G. (1990). A new approach to high-efficiency multi-band-gap solar cells. Journal of Applied Physics, 67(7), 3490–3493. https://doi.org/10.1063/1.345339

Bati, A. S. R., Zhong, Y. L., Burn, P. L., Nazeeruddin, M. K., Shaw, P. E., & Batmunkh, M. (2023). Next-generation applications for integrated perovskite solar cells. Communications Materials, 4(1). https://doi.org/10.1038/s43246-022-00325-4

Benesperi, I., Michaels, H., & Freitag, M. (2018). The researcher's guide to solid-state dye-sensitized solar cells. Journal of Materials Chemistry C, 6(44), 11903–11942. https://doi.org/10.1039/c8tc03542c

Bi, Z., Zhang, J., Zheng, Q., Lv, L., Lin, Z., Shan, H., Li, P., Ma, X., Han, Y., & Hao, Y. (2016). An InGaN-Based Solar Cell Including Dual InGaN/GaN Multiple Quantum Wells. IEEE Photonics Technology Letters, 28(20), 2117–2120. https://doi.org/10.1109/lpt.2016.2575058

Biswas, P., Hasan, A. S., Rahim, A. B., Ullah, A., & Chowdhury, I. B. (2015). Analytical approach of J-V characteristics of CdTe based thin film solar cells including voltage and space dependent electric field in the absorber layer. 2nd International Conference on Electrical Information and Communication Technologies (EICT), 446–450. https://doi.org/10.1109/eict.2015.7391994

Chakma, N., Dey, G., Huda, N., Asaduzzaman, M., Chowdhury, M. H. D., Chowdhury, M. R. H., Islam, M. J., & Chowdhury, I. B. (2024, October 14). A Silvaco TCAD Approach of Performance Analysis of P3HT-Based Organic Solar Cell. https://matjournals.net/engineering/index.php/JAEED/article/view/1014

Chen, Y., Zhang, M., Li, F., & Yang, Z. (2023). Recent Progress in Perovskite Solar Cells: Status and Future. Coatings, 13(3), 644. https://doi.org/10.3390/coatings13030644

Chowdhury, M. I., Islam, M. J., & Arif, M. I. H. (2020, March 28). Internal Quantum Efficiency of Hydrogenated Amorphous Silicon Based Plasmonic Thin Film Solar Cells Using Photonic Crystal Back Reflectors. https://matjournals.co.in/index.php/JEPSE/article/view/2988

Chowdhury, M. I., & Mostafa, M. J. I. S. (2020, February 24). SILVACO TCAD Implementation of Dual Junction Quantum Well Solar Cell. https://matjournals.co.in/index.php/JOARES/article/view/3683

Chowdhury, M. R. H., Chowdhury, M. H. D., Islam, M. J., & Chowdhury, I. B. (2024, November 21). SILVACO TCAD Based Investigation of P3HT: PCBM-Based Bulk Heterojunction Organic Solar Cell. https://matjournals.net/engineering/index.php/JIIS/article/view/1113

Chowdhury, T. A., Zafar, M. a. B., Islam, M. S., Shahinuzzaman, M., Islam, M. A., & Khandaker, M. U. (2023). Stability of perovskite solar cells: issues and prospects. RSC Advances, 13(3), 1787–1810. https://doi.org/10.1039/d2ra05903g

Chowdhury, W. H., Sara, Z. A., Miah, M. M., Das, M., & Chowdhury, M. I. B. (2021). Efficiency Enhancement of a PCDTBT/PC71 BM-based Organic Solar Cell Through Layer-thickness Optimization. 2021 2nd International Conference on Robotics, Electrical and Signal Processing Techniques (ICREST), 684–688. https://doi.org/10.1109/icrest51555.2021.9331006

Guillemoles, J., Kirchartz, T., Cahen, D., & Rau, U. (2019). Guide for the perplexed to the Shockley–Queisser model for solar cells. Nature Photonics, 13(8), 501–505. https://doi.org/10.1038/s41566-019-0479-2

Haque, M. M., Rahman, M. M., & Chowdhury, M. I. B. (2014a). Current-voltage characteristics of CdS/CIGS thin film solar cells: An analytical approach. In 1st International Conference on Non Conventional Energy (ICONCE 2014) (pp. 24–27). https://doi.org/10.1109/iconce.2014.6808695

Haque, M. M., Rahman, M. M., & Chowdhury, M. I. B. (2014b). Current-voltage characteristics of CdS/CdTe thin film solar cells: An analytical approach. 3rd International Conference on the Developments in Renewable Energy Technology (ICDRET), 18, 1–4. https://doi.org/10.1109/icdret.2014.6861729

Hasan, M. M., & Chowdhury, M. I. B. (2018, December 31). Modelling and Analysis of CdS/CZTSSe Based Thin Film Solar Cell. https://xpublication.com/index.php/jmo/article/view/220

Herz, L. M. (2017). Charge-Carrier Mobilities in Metal Halide Perovskites: Fundamental Mechanisms and Limits. ACS Energy Letters, 2(7), 1539–1548. https://doi.org/10.1021/acsenergylett.7b00276

Ho, S., Chowdhury, H. D., MD, Chowdhury, M. R. H., & Chowdhury, M. I. B. (2024). Recent Advances in the Development of Organic Solar Cells and Perovskite Solar Cells. International Journal of Engineering Trends and Technology, 72(9), 139–153. https://doi.org/10.14445/22315381/ijett-v72i9p112

Hossain, M., Ahmed, K., Rubyat, K. M., Chowdhury, M. H. D., Chowdhury, M. R. H., Islam, M., & Chowdhury, M. I. B. (2014). Simulation-Driven Fabrication and Performance Evaluation of n-MOSFET using Silvaco Athena and Atlas: From Process to Parameters. Journal of Microprocessor and Microcontroller Research., 1(3), 21–43. https://doi.org/10.46610/jommr.2024.v01i03.003

Huqe, M. R., Aziz, H. M., Kolince, K. M., Uddin, M. S., & Chowdhury, M. I. B. (2012). Effect of ge-dosing profile of exponentially-doped base on the internal quantum efficiency of a SiGe solar cell. In International Conference on Devices, Circuits and Systems (ICDCS) (pp. 119–123). https://doi.org/10.1109/icdcsyst.2012.6188686

Huqe, M. R., & Chowdhury, M. I. B. (2016). Internal quantum efficiency of Si-drift solar cells with nonuniformly and heavily doped emitter. In 4th International Conference on the Development in the in Renewable Energy Technology (ICDRET). https://doi.org/10.1109/icdret.2016.7421523

Huqe, M. R., Reba, S. İ., Uddin, M. S., & Chowdhury, M. İ. B. (2013, June 1). Analytical Modeling of the Base Dark Saturation Current of Drift-Field Solar Cells Considering Auger Recombination. https://dergipark.org.tr/en/pub/ijrer/issue/16079/168254

Husainat, A., Ali, W., Cofie, P., Attia, J., & Fuller, J. (2019). Simulation and analysis of methylammonium lead iodide (CH3NH3PBI3) perovskite solar cell with AU contact using SCAPS 1D simulator. American Journal of Optics and Photonics, 7(2), 33. https://doi.org/10.11648/j.ajop.20190702.12

Islam, A., & Chowdhury, M. I. B. (2014). A simulink based generalized model of PV cell / array. In 3rd International Conference on the Developments in Renewable Energy Technology (ICDRET) (pp. 1–5). https://doi.org/10.1109/icdret.2014.6861683

Islam, M. J., Chowdhury, M. H. D., Chowdhury, M. R. H., & Chowdhury, I. B. (2024, September 6). Investigation of Improved Performance of ZnO/CIGS-Based Solar Cells. https://matjournals.net/engineering/index.php/JAEED/article/view/911

Islam, M. J., & Chowdhury, M. I. B. (2024, July 29). Investigation of an InGaN Based Quantum Well Solar Cell Using Silvaco TCAD. https://matjournals.net/engineering/index.php/JAEED/article/view/694

Islam, M. J., Hasan, M. M., Sami, R., & Chowdhury, M. I. B. (2016). Modeling of graphene/SiO2/Si(n) based metal-insulator-semiconductor solar cells. In 4th International Conference on the Development in the in Renewable Energy Technology (ICDRET) (pp. 1–4). IEEE. https://doi.org/10.1109/icdret.2016.7421491

Islam, M. J., Mostafa, S., & Chowdhury, M. I. B. (2020). Thickness Optimization of Single Junction Quantum well Solar Cell Using TCAD. International Journal of Engineering and Technologies, 18, 1–7. https://doi.org/10.56431/p-rq2260

Islam, M. N., Chowdhury, M. R. H., Chowdhury, M. H. D., Islam, M. J., Rahaman, M. L., & Chowdhury, M. I. B. (2024). A High-Efficiency Dye-Sensitized Solar Cell Using PCDTBT:PCBM as Solid Electrolyte and Graphene Oxide as Hole Transport Layer. In 6th International Conference on Electrical Engineering and Information & Communication Technology (ICEEICT) (pp. 933–938). https://doi.org/10.1109/iceeict62016.2024.10534413

Jeon, N. J., Na, H., Jung, E. H., Yang, T., Lee, Y. G., Kim, G., Shin, H., Seok, S. I., Lee, J., & Seo, J. (2018). A fluorene-terminated hole-transporting material for highly efficient and stable perovskite solar cells. Nature Energy, 3(8), 682–689. https://doi.org/10.1038/s41560-018-0200-6

Johir, M. J. I., Arif, M. I. H., Mostafa, S., Nadeem, M., Hasan, M. M., Habib, K., & Chowdhury, M. I. B. (2021, January 28). Investigation of Quantum Efficiency of GaAs/InAs-Based Quantum Well Solar Cell. https://matjournals.co.in/index.php/JIIS/article/view/2638

Kabir, E., Kumar, P., Kumar, S., Adelodun, A. A., & Kim, K. (2017). Solar energy: Potential and future prospects. Renewable and Sustainable Energy Reviews, 82, 894–900. https://doi.org/10.1016/j.rser.2017.09.094

Kojima, A., Teshima, K., Shirai, Y., & Miyasaka, T. (2009). Organometal Halide Perovskites as Visible-Light Sensitizers for Photovoltaic Cells. Journal of the American Chemical Society, 131(17), 6050–6051. https://doi.org/10.1021/ja809598r

Mostafa, S., Nadeem, M., Arif, M. I. H., Islam, M. J., & Chowdhury, M. I. B. (2020). Performance Optimization of Quantum Well Solar Cells Through Layer Thickness Variation. In 23rd International Conference on Computer and Information Technology (ICCIT) (pp. 1–6). https://doi.org/10.1109/iccit51783.2020.9392741

Murugesan, V. S., Ono, S., Tsuda, N., Yamada, J., Shin, P., & Ochiai, S. (2015). Characterization of Organic Thin Film Solar Cells of PCDTBT : PC71BM Prepared by Different Mixing Ratio and Effect of Hole Transport Layer. International Journal of Photoenergy, 2015, 1–8. https://doi.org/10.1155/2015/687678

Nabiah, S. N., Islam, M. J., & Chowdhury, M. I. B. (2024, July 10). Silvaco TCAD Implementation of All-InGaN Based Quantum Well Solar Cell. Nabiah | Journal of Advancement in Communication System. http://hbrppublication.com/OJS/index.php/JACS/article/view/5765

Nawaz, S. S., Haque, F. N. N., & Chowdhury, M. I. B. (2023, January 5). Silvaco TCAD Implementation of GaAs/GaSb Quantum Dot Solar Cell. Nawaz | Advancement of Signal Processing and Its Applications. http://hbrppublication.com/OJS/index.php/ASPIA/article/view/2872

Nayak, P. K., Mahesh, S., Snaith, H. J., & Cahen, D. (2019). Photovoltaic solar cell technologies: analysing the state of the art. Nature Reviews Materials, 4(4), 269–285. https://doi.org/10.1038/s41578-019-0097-0

Nikita, K. N., Gaffar, M. A., & Chowdhury, M. I. B. (2016). Exploring the opportunity of using graphene as the transparent conducting layer in CZTS-based thin film solar cells. In 3rd International Conference on Electrical Engineering and Information Communication Technology (ICEEICT). https://doi.org/10.1109/ceeict.2016.7873130

Nowsherwan, G. A., Iqbal, M. A., Rehman, S. U., Zaib, A., Sadiq, M. I., Dogar, M. A., Azhar, M., Maidin, S. S., Hussain, S. S., Morsy, K., & Choi, J. R. (2023). Numerical optimization and performance evaluation of ZnPC:PC70BM based dye-sensitized solar cell. Scientific Reports, 13(1). https://doi.org/10.1038/s41598-023-37486-2

O'Regan, B., & Grätzel, M. (1991). A low-cost, high-efficiency solar cell based on dye-sensitized colloidal TiO2 films. Nature, 353(6346), 737–740. https://doi.org/10.1038/353737a0

Park, J., Kim, J., Yun, H., Paik, M. J., Noh, E., Mun, H. J., Kim, M. G., Shin, T. J., & Seok, S. I. (2023). Controlled growth of perovskite layers with volatile alkylammonium chlorides. Nature, 616(7958), 724–730. https://doi.org/10.1038/s41586-023-05825-y

Pitaro, M., Tekelenburg, E. K., Shao, S., & Loi, M. A. (2021). Tin Halide Perovskites: From Fundamental Properties to Solar Cells. Advanced Materials, 34(1). https://doi.org/10.1002/adma.202105844

Rahim, A. B., Hasan, A. S., Biswas, P., Ullah, A., & Chowdhury, M. I. B. (2015). Analytical modeling of J-V characteristics of CIGS based thin film solar cell considering voltage and space dependent electric field in the absorber layer. In International Conference on Advances in Electrical Engineering (ICAEE) (pp. 368–371). https://doi.org/10.1109/icaee.2015.7506871

Rahman, S., Haleem, A., Siddiq, M., Hussain, M. K., Qamar, S., Hameed, S., & Waris, M. (2023). Research on dye sensitized solar cells: recent advancement toward the various constituents of dye sensitized solar cells for efficiency enhancement and future prospects. RSC Advances, 13(28), 19508–19529. https://doi.org/10.1039/d3ra00903c

Reference Air Mass 1.5 Spectra. (n.d.). Grid Modernization | NREL. https://www.nrel.gov/grid/solar-resource/spectra-am1.5.html

RefractiveIndex.INFO - Refractive index database. (n.d.). https://refractiveindex.info/

Rivon, S. A., Biswas, P., Hasan, A. S., Rahim, A. B., & Chowdhury, M. I. B. (2016). Analytical modelling of Cds/CdTe based thin film solar cells considering surface recombination. 3rd International Conference on Electrical Engineering and Information Communication Technology (ICEEICT), 1–5. https://doi.org/10.1109/ceeict.2016.7873135

Saha, N. S. K., Ferdaus, N. S. I., Farhan, N. a. M., Reba, N. S. I., & Chowdhury, N. M. I. B. (2011). Effect of field dependent mobility on the analytical modeling of emitter saturation current of a silicon solar cell. In International Conference on Computer Applications and Industrial Electronics (ICCAIE) (Vol. 20, pp. 7–11). IEEE. https://doi.org/10.1109/iccaie.2011.6162094

Saha, S. K., Farhan, A. M., Reba, S. I., Ferdaus, S. I., & Chowdhury, M. I. B. (2011). An analytical model of dark saturation current of silicon solar cell considering both SRH and Auger recombination. IEEE Regional Symposium on Micro and Nanoelectronics, 9–13. https://doi.org/10.1109/rsm.2011.6088280

Saha, S. K., Ferdaus, S. I., Reba, N. S. I., & Chowdhury, M. I. B. (2011). Effect of field dependent mobility and simultaneous consideration of both SRH and auger recombination on the analytical modeling of internal quantum efficiency of a si-solar cell. In TENCON 2011 - 2011 IEEE Region 10 Conference. IEEE. https://doi.org/10.1109/tencon.2011.6129190

Tebbal, I., & Hamida, A. F. (2023). Effects of Crossover Operators on Genetic Algorithms for the Extraction of Solar Cell Parameters from Noisy Data. Engineering Technology & Applied Science Research, 13(3), 10630–10637. https://doi.org/10.48084/etasr.5417

Wu, J., Cha, H., Du, T., Dong, Y., Xu, W., Lin, C., & Durrant, J. R. (2021). A Comparison of Charge Carrier Dynamics in Organic and Perovskite Solar Cells. Advanced Materials, 34(2). https://doi.org/10.1002/adma.202101833